

## Thermal Behavior of Cathode Bottom Lining at CBA

Dagoberto S. Severo<sup>1</sup>, Henrique C. dos Santos<sup>2</sup>, Jefferson L. dos Santos<sup>3</sup> and Fabio N. M. de Carvalho<sup>4</sup>

1. Director, CAETE Engenharia Ltda, Porto Alegre, RS, Brazil

2. Process Consultant

3. Process Engineer

4. Production Engineer

Companhia Brasileira de Alumínio (CBA), Alumínio, SP, Brazil

Corresponding author: dagoberto@caetebr.com

### Abstract

The heat dissipation at the cell bottom represents 7 - 20 % of the total aluminium smelting cell heat losses, depending on lining design and its condition. The heat transfer at the bottom region is controlled by the thermal insulation of materials. Insulation bricks can be attacked by sodium and bath components, if proper conditions for their diffusion are met, causing deterioration of the material insulation properties. Thermal measurements of the cell bottom insulation evolution with age were made for the existing CBA cell lining, showing progressive increment on heat losses along the lining life. High bottom heat losses not only require more voltage to keep the cell in thermal balance, increasing energy consumption, but also may induce sludge formation on the cathode panel. This increases cathode voltage drop, perturbs horizontal currents in the metal and consequently increases MHD instability. As a solution, a stainless-steel barrier was installed in ten test cells to prevent bath components and sodium migration into the insulation bricks. Heat flow measurement surveys were done to assess the steel barrier efficiency relative to thermal energy saving over time.

**Keywords:** Lining design, cathode sludge, diffusion barrier, lining ageing, cell heat losses.

### 1. Introduction

The region below the carbon cathode block is called sub-cathodic and modern designs have layers of refractory and insulation bricks or slabs. The function of the refractory bricks is to protect the insulation underneath. This is because during cell operation sodium and bath percolates through the cathode block towards the shell bottom.

A typical cross section of a used lining, as shown in Figure 1, presents a layer called “build-up” of white grey colour consisting of cryolite, sodium fluoride, aluminium, alumina, silicon,  $Al_4C_3$ , Fe-Si and Fe-Al alloys. Below this layer there is a dense black layer consisting of reacted refractory where nepheline ( $NaAlSiO_4$ ) and a glassy phase close to albite ( $NaAlSi_3O_8$ ) were found [1]. This layer acts as a diffusion barrier slowing down further sodium and bath penetration. The sharp interface between the intact refractory brick and this layer is what is called “reaction front”. The solidus temperature of this front, if albite is present in addition of sodium fluorite and cryolite, is around 865 °C [1]. By design, this isotherm should be located within the refractory brick, not in the insulation layer.

However, the percolation of bath through the cathode block will not stop during the cell life. The consequence will be accumulation of material below the cathode, the “build-up”. This may result in lift of the cathode panel, the “heave”, and/or compression of insulation material that will move the solidification isotherm downwards, thus progressing the contamination.

The refractories used are aluminosilicate chamotte bricks with high silica content since it was found to have a better cryolite resistance [2], most likely because it results in a more viscous glass diffusion barrier.

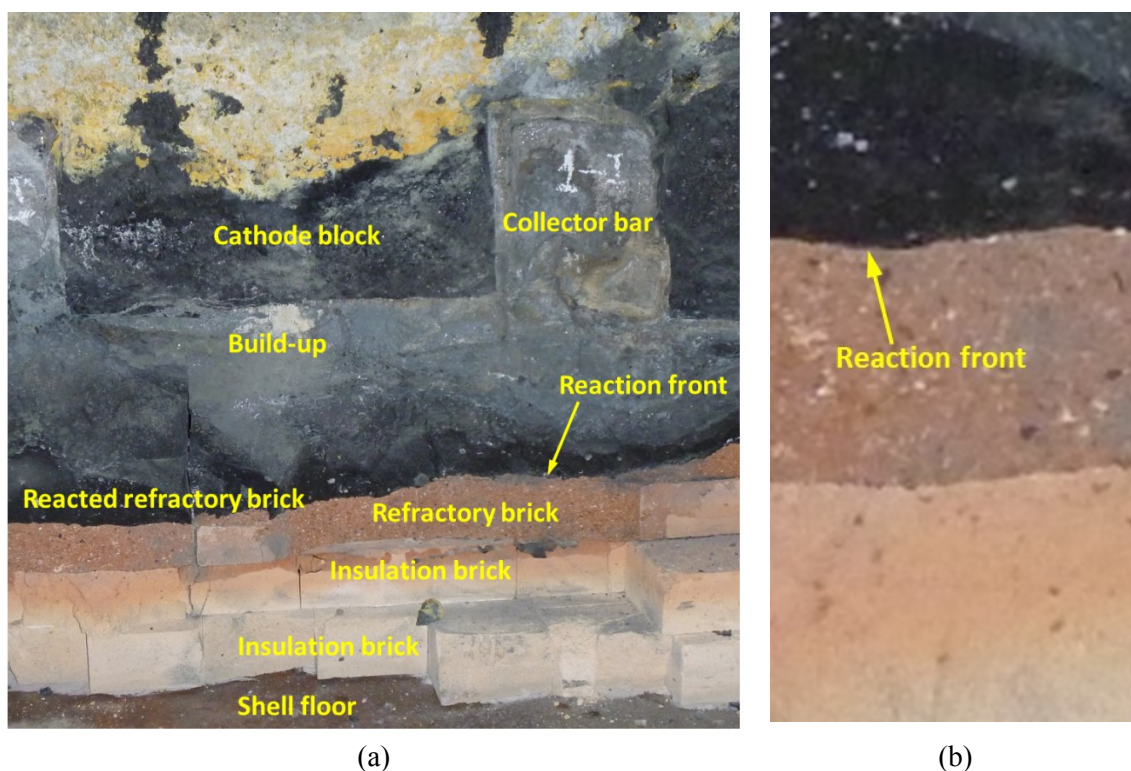


**Figure 1. Cell cross section bottom lining (a) and reaction front in detail (b).**

There is a fine balance in a well-designed bottom lining for aluminium reduction cells. The thermal resistance of the bottom should be high enough to provide good energy efficiency but at the same time, it should not be too high to favour the sodium and bath contamination which deteriorates the insulation over time.

In the case of an over-insulated bottom design, in the beginning of the cell life a too high temperature at the hot face of the insulation layer would be present, reacting with percolating bath components and being destroyed completely too early in the pot life. When the insulation is destroyed, its thermal conductivity increases reducing the bottom thermal resistance which will in turn increase heat losses, thus reducing process energy efficiency. Also, sludge and bottom freeze may become an issue, requiring more heat generation.

In a bottom with a thermal resistance designed to have the solidification isotherm inside the refractory bricks, the heat flux is a little higher but stable over time and it is not necessary to increase cell voltage to compensate extra heat losses. Figure 2 shows the heat flux measurements for two different lining designs of the same technology that relies only on high silica refractories as diffusion barrier. Lining A is the old design with theoretical thermal resistance of  $1.24 \text{ m}^2\text{K/W}$ , which results in an initial heat flux of  $680 \text{ W/m}^2$ . However, the insulation hot face temperature is  $877^\circ\text{C}$  leading to its deterioration over time. Lining B was designed to have a thermal resistance of  $0.84 \text{ m}^2\text{K/W}$ , having an initial heat flux of  $980 \text{ W/m}^2$ , but in this case the insulation hot face temperature is  $810^\circ\text{C}$ . The heat flux remains stable over the period of 600 days when the Lining A was already having more than twice the designed heat flux.

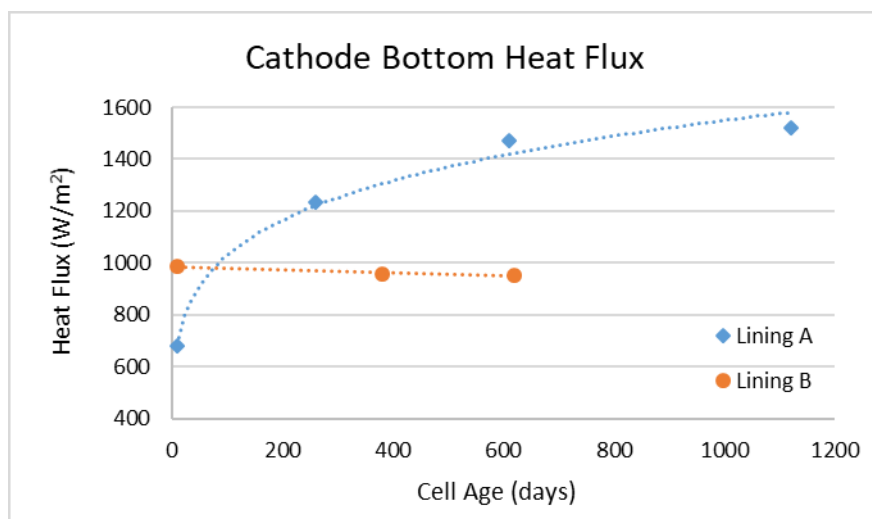


**Figure 2. Cathode bottom heat flux against cell age.**

Figure 3 shows the sub-cathodic lining autopsy of a Lining B cell design at the age of 1300 days which failed due to sidewall problems. It can be noted that the two insulation brick layers were not contaminated. Also, one of the 3 refractory layers is still intact.



**Figure 3. Cell lining cross section of Lining B design.**

## 2. CBA Sub-Cathodic Design

Presently, the cells at CBA are running at 130 kA and use graphitized cathode blocks. The average cathode cell life is very good and was 2 800 days with 650 days of standard deviation in 2017. Also, the energy efficiency of CBA cells, considering a Soderberg technology, is quite good and around 14.4 kWh/kg Al.

### 2.1 Existing Bottom Lining Design

The CBA existing bottom lining design has 2 layers of refractories and three layers of molar insulation bricks, with the top layer having higher density. Figure 4 (b) shows a cross section of the bottom design versus temperature achieved. The 3D electro-thermal numerical model, as shown in Figure 4 (a), using dimensions and material properties unchanged (not contaminated), results in a theoretical bottom thermal resistance of 1.07 m<sup>2</sup>K/W. This results in an insulation hot face temperature of 860 °C, a shell temperature of 109 °C and bottom heat flux of 790 W/m<sup>2</sup>.

The refractory bricks used by CBA were provided from a local supplier and although the datasheet specified 56 % of SiO<sub>2</sub>, tests conducted by CBA have found only 47 – 52 %.

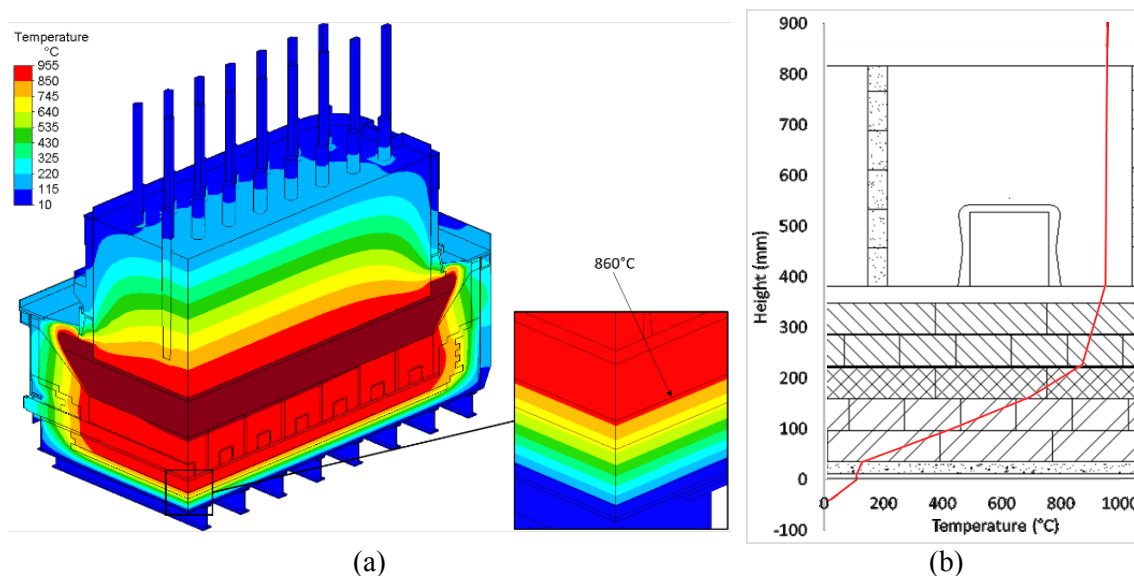


**Figure 4. CBA cell thermal model results.**

In February 2013, an autopsy was made in the cell 1639 with 3065 days of life. A cross section in the middle of the cell, at cathode 7 position, is shown in Figure 5.



**Figure 5. CBA cell lining cross section – Cell 1639 autopsy.**

Figure 6 shows other cathode positions for the same cell. We can see the affected refractories (black glassy), but the reaction front is not sharp. Also, below the front we can see that the insulation bricks are contaminated in a non-uniform way. Since the cell is very old we can see a lot of build-up just below the cathode (white grey). The cathode block bottom position was measured during the autopsy and there was 150 mm of build-up thickness in average. The insulation bricks were not compressed.

More information about the cathode performance and autopsies at CBA was published by Pardo [3].



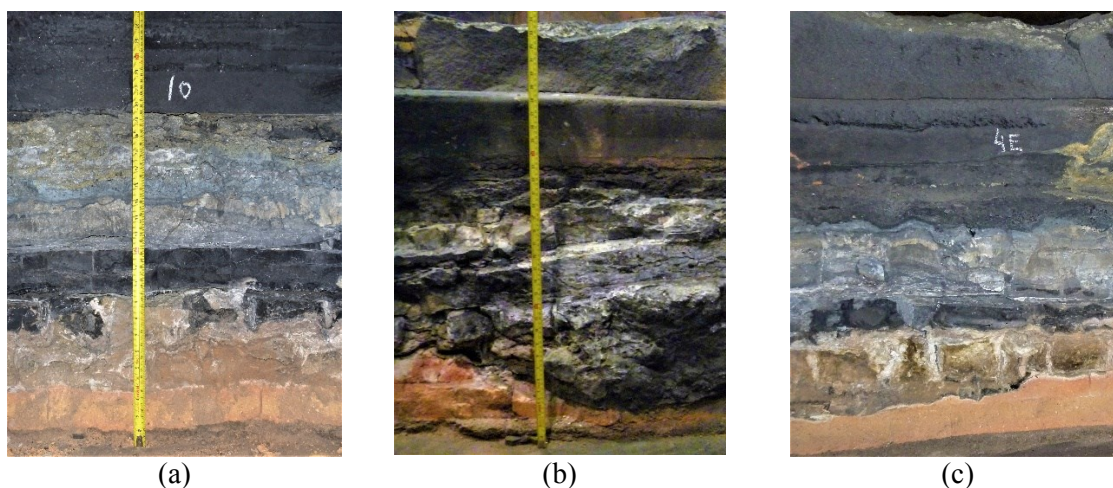


**Figure 6. CBA cell bottom lining details – Cell 1639 autopsy.**

## 2.2 Test Cells Bottom Lining Design

In order to solve the diffusion barrier issue found in the autopsy and models, a steel plate barrier was proposed. As shown by Allaire [4], low carbon steel plates in a cell tend to convert to iron oxide thus losing its sodium barrier effectivity. Stainless steel AISI 304 was chosen believing that it may survive longer than low carbon steel. The plates were installed just above the insulation brick layer - Figure 7 (a). Also, due to its non-magnetic property the plates were safely installed in the presence of the magnetic field inside the potroom as shown in Figure 7 (b). Ten test cells were built from June to December 2015.

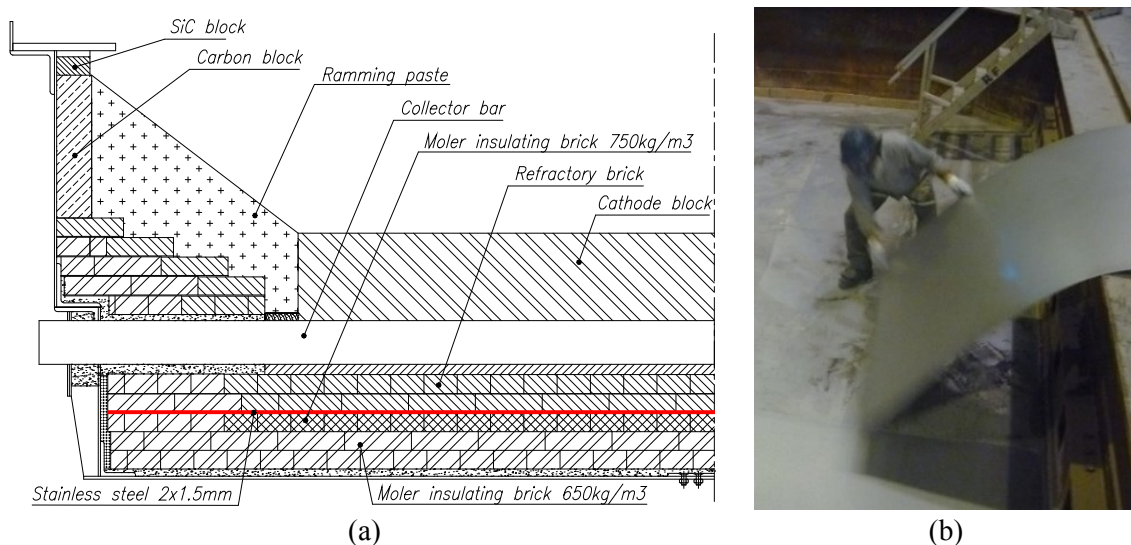


**Figure 7. New lining design (a) and stainless steel plates being installed (b).**

## 3. Temperature Measurements

In order to check the temperature at the insulation hot face during operation, thermocouples were installed just below the steel plates, as shown in Figure 8. Different cathode positions were chosen and 2 to 3 thermocouples were installed in each one of the 10 test cells.

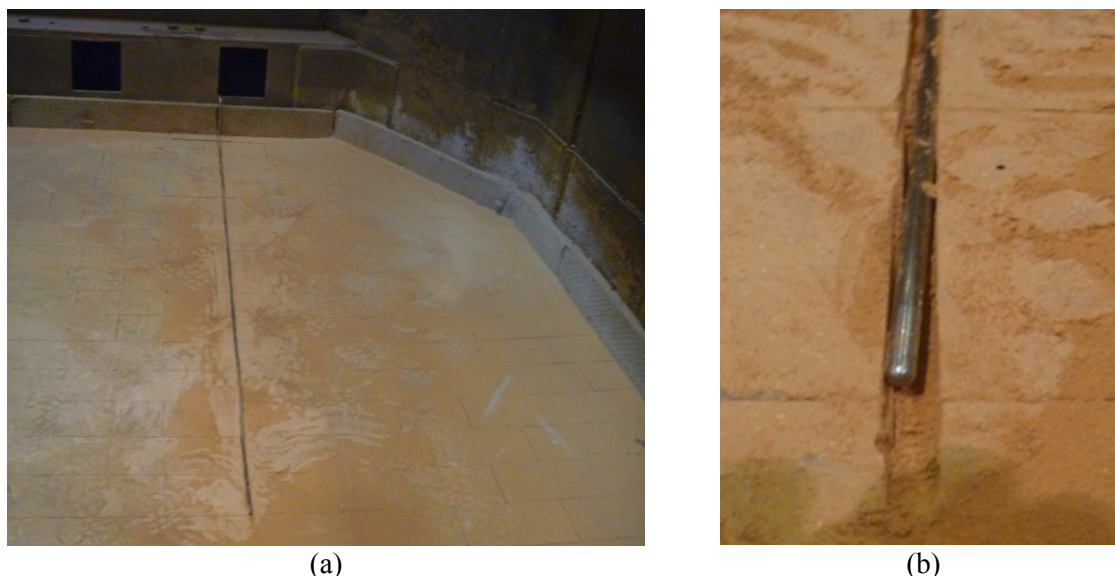


**Figure 8. Thermocouple installed in the hot face of the insulation (a) and detail (b).**

The Figure 9 shows the results of these measurements in the first 8 months of cell life. It is possible to notice some dispersion in the obtained values. In the beginning, the values range from 850 – 885 °C, reducing to around 820 – 865 °C within 30 days and stabilizing in 820 – 850 °C within around 90 days.

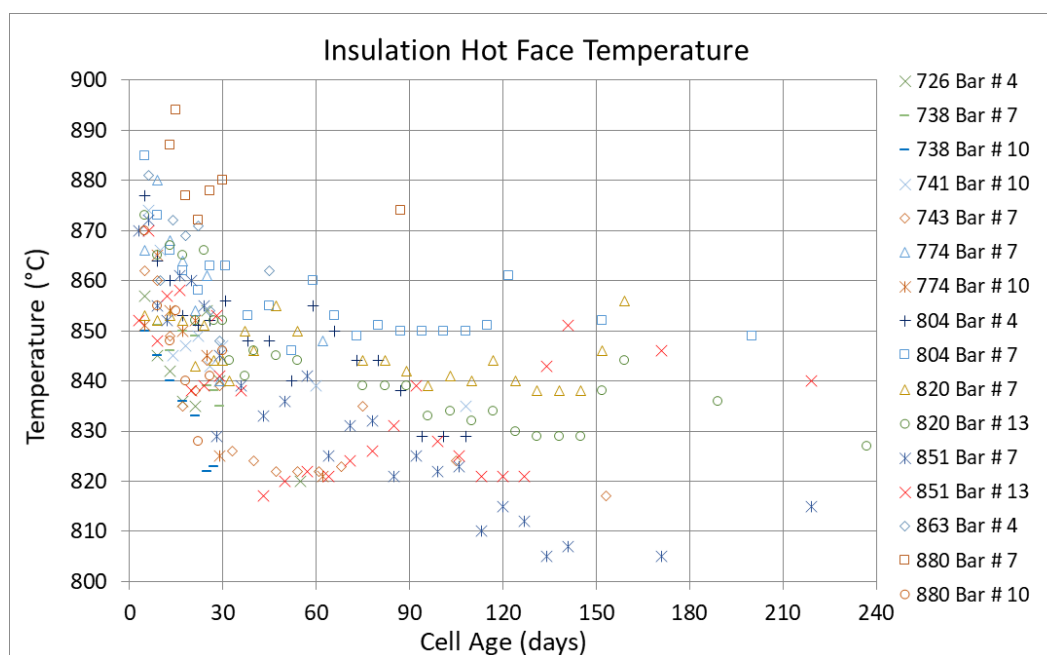


**Figure 9. Insulation bricks hot face temperature in the test cells. The numbers on the right are test cell numbers.**

Figure 10 shows the bath temperature measurements taken at the same time as the lining thermocouples. We can see that the temperature remains high over the initial 30 days of the cell life, reflecting in the insulation temperature.

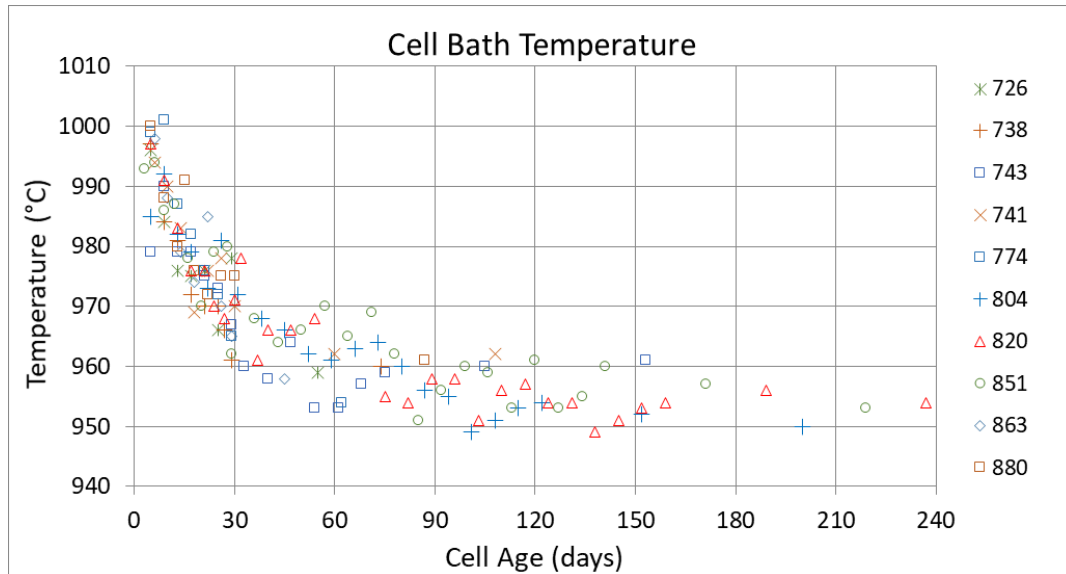


Figure 10. Bath temperature in the test cells.

#### 4. Heat Flux Measurements

##### 4.1 Sensor

The heat flux sensor is a thin plate made of a material with a known low thermal conductivity having differential thermocouples over the sensor area – Figure 11 [5]. The temperature difference between the two faces is used to calculate the heat flux passing through the sensor by applying the Fourier law (Equation 1).

$$\phi_q = -k \frac{dT}{dx} = -k \frac{T_2 - T_1}{D} \quad (1)$$

where:

- $\phi_q$  Heat flux, W/m<sup>2</sup>
- $k$  Thermal conductivity, W/m.K
- $T$  Temperature, °C
- $T_2$  Temperature at the hot face of the plate, °C
- $T_1$  Temperature at the cold face of the plate, °C
- $x$  Coordinate through the plate thickness, m
- $D$  Distance between thermocouple layers.

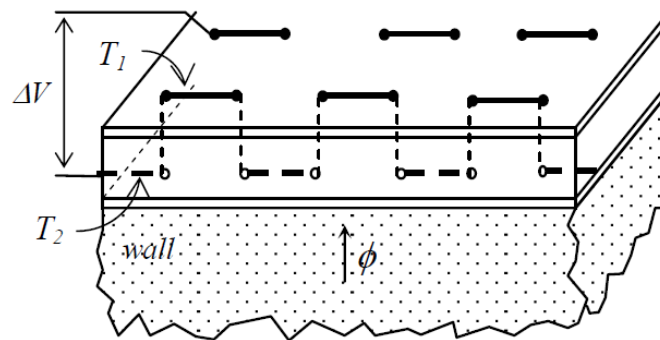
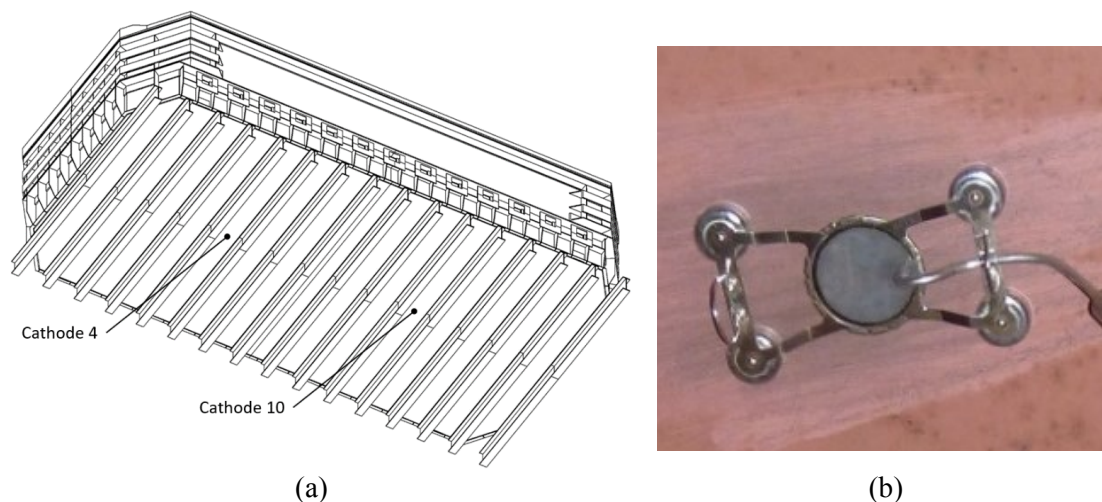


Figure 11. Typical heat flux sensor – reproduced from [5].

The heat flux is measured by attaching the sensor to the surface of interest. A good contact between sensor and surface should be guaranteed with no air pockets between them. Also, surface finishing and planarity are important to consider. The installation of the sensor itself on the surface disturbs the heat flux crossing it. The main difficulty is found when the local condition is windy. This is because the wind locally cools down the sensor which shows larger fluctuations than the real one to be measured. Even with steady wind, the sensor will show a higher value than the actual flow. This is due to the difference of the sensor transfer constant which was calibrated in no wind condition.

## 4.2 Measurements

Heat flux and temperature were measured at the shell bottom between cradles as shown in Figure 12. The positions were just below cathodes 4 and 10. The goal was to assess the behaviour over the pot life. Figure 12 (b) shows the KEM (Kyoto Electronics Manufacturing) T500B sensor in use on the steel potshell. The existing bottom design cells were selected to have different ages.



**Figure 12. Heat flux sensor position (a) and view of the sensor used (b).**

Figure 13 shows the measurements of heat flux on three occasions (2015, 2016 and 2018) for cells of the existing bottom lining design and the test cells using stainless steel (Inox) plates. We can see the somewhat high dispersion of the values measured in the existing bottom lining cells and there is no clear correlation between heat flux and age. Although some of the older cells give values close to the theoretical initial value of  $790 \text{ W/m}^2$ , most of them show higher values, including some younger cells. The test cells show a much more uniform behaviour and their heat flux did not increase until the age of 1100 days. The only exception was Cell 851, which had a metal tap-out through the collector bars on 12 and 13 in July 2018.

The presence of liquid or solid sludge on the top of the cathode may explain the low heat flux values for the existing design older cells.

Figure 14 shows the cell bottom temperature measurements. The behaviour is very similar to the heat flux. Again, the hottest test cell in 2018 is the 851.

The bottom insulation is uniform by design and no difference should exist between cathode 4 and 10 positions. Figure 15 shows the absolute heat flux difference between the cathodes 4 and 10. The difference may be an indication that part of the lining has deteriorated. The test cells



present less variation except for the Cell 851 which had an episode of collector bar metal tap-out that might have resulted in the partial destruction of the steel plates.

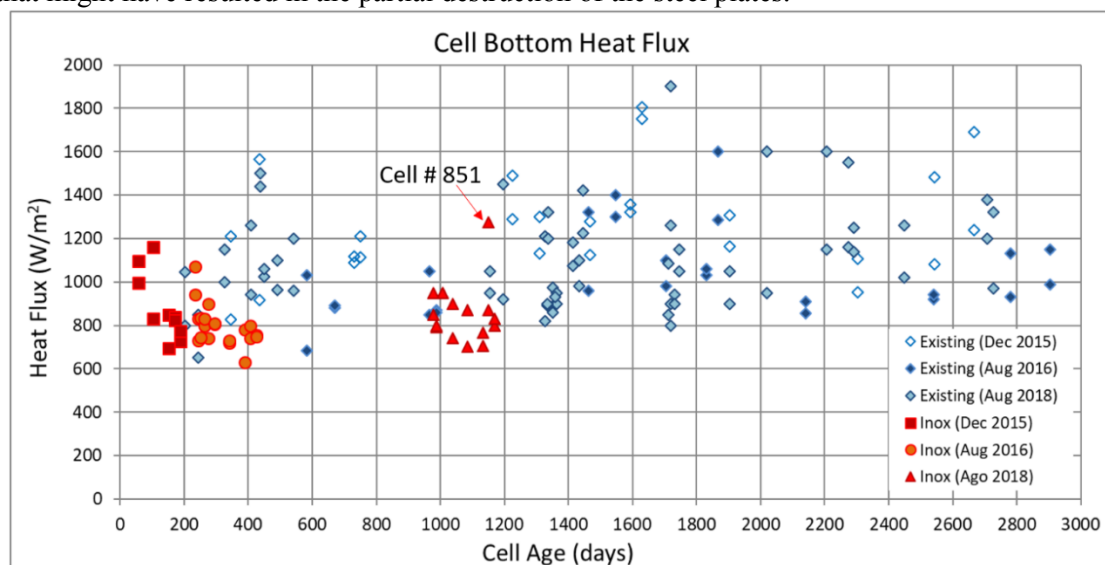


Figure 13. Cell bottom heat flux measurements.

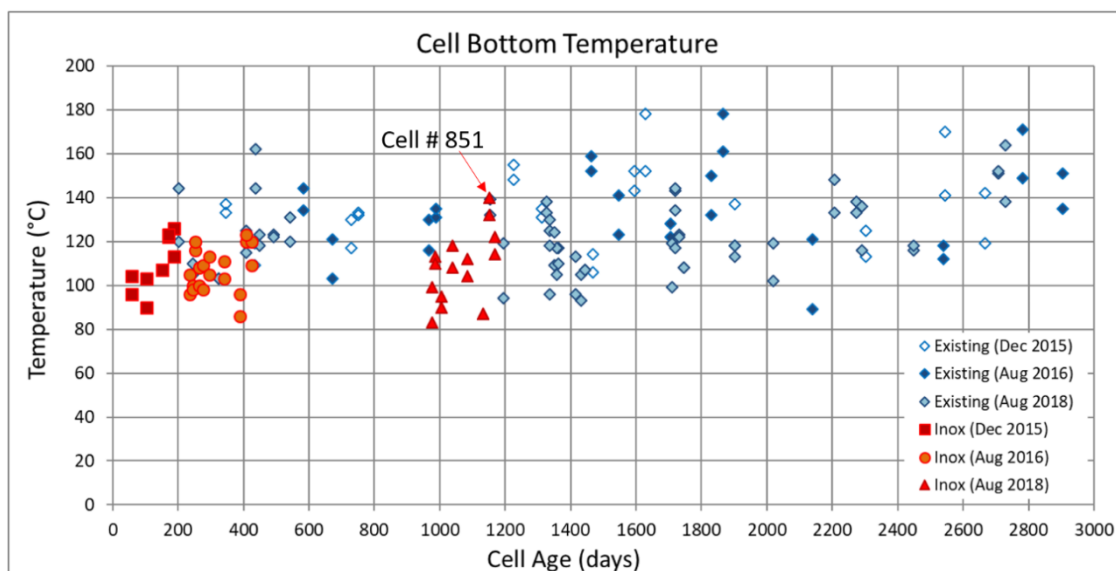
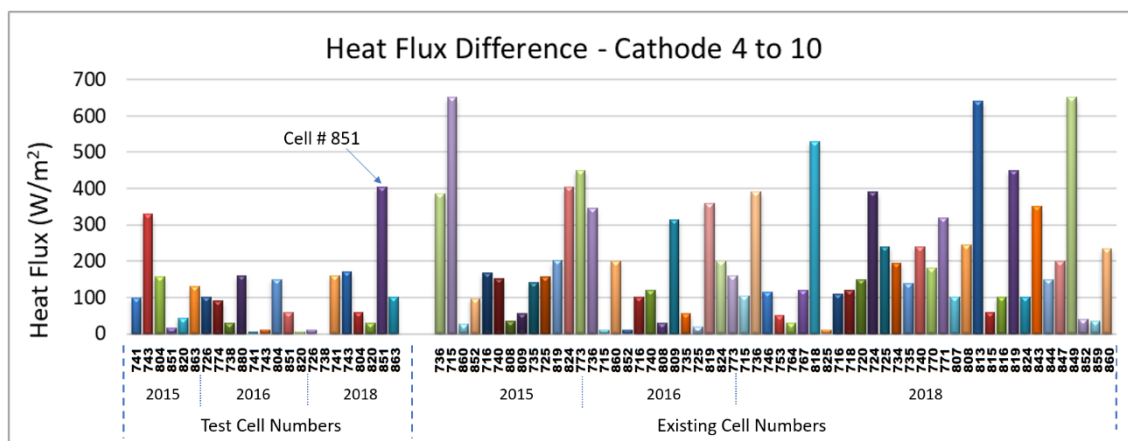
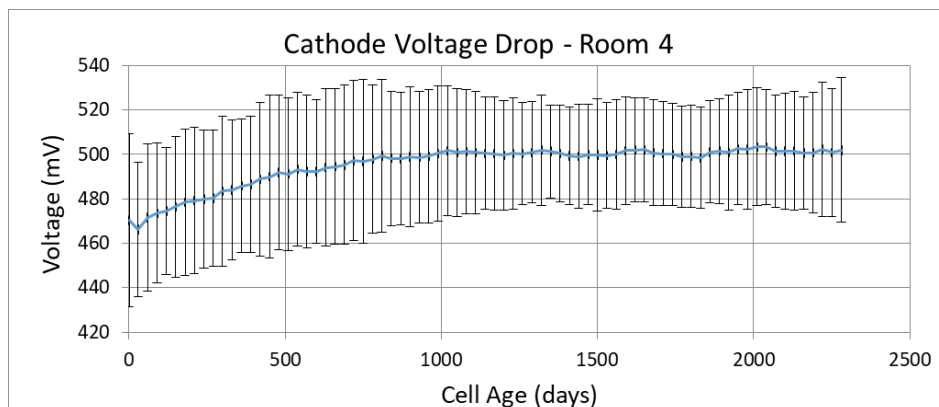


Figure 14. Bottom temperature measurements.



**Figure 15. Bottom heat flux absolute difference between cathode 4 and 10 positions.****5. Cell Voltage**

Cell voltage is a function of the electrical resistance of the circuit between identical positions in two adjacent cells. Busbar and anode resistances are almost constant. Cathode resistance is different from cell to cell and also is changing in time due to the increase in contact resistance, cracks and material properties. Figure 16 shows the measured cathode voltage drop (including 235 mV of busbar drop) over time for CBA Room 4. The value starts around 460 mV and becomes stable after 800 days at around 500 mV, with a standard deviation of around 25 mV.

**Figure 16. Cathode voltage drop over life for all cells in Room 4 (8 December 2015).**

The increase in cathode voltage drop over the cell life has no impact on the total cell voltage to maintain the heat balance if the cell voltage is kept constant. This is because it makes no difference where the heat is generated - whether in the cathode or in the anode-cathode distance (ACD). The increase in cathode voltage results in a decrease in ACD [6]. Our models (@129 kA) show that for an increase in cathode voltage drop from 460 to 500 mV, the ACD has to be reduced by 1.5 mm. The negative impact of lower ACD could be lower current efficiency due to metal re-oxidation and higher magnetic instability if the ACD limit is reached. The total voltage being the same, the thermal balance is kept the same and the heat loss through the external surfaces remains the same.

However, the required cell voltage should increase over cell life due to increased thermal losses by the lining as it deteriorates. The increase in thermal losses requires more heat generation through the ACD which results in more voltage to maintain the thermal balance. Figure 17 shows the theoretical extra voltage to be added to compensate for this increase and keep the cell in heat balance for the existing design cells measured. We considered 790 W/m<sup>2</sup> as the reference bottom heat loss at the beginning of the cell life before the contamination of the insulation. There is 80 mV extra voltage in average, but the dispersion is high and, as for the heat flux, there is a weak correlation between extra voltage and cell life.

Figure 18 shows the total cell voltage as a function of cell life in two different days for all cells in Room 4. There is no correlation between cell life and voltage meaning that current efficiency and/or superheat are being affected in the old cells that have the bottom lining deteriorated and the cathode voltage drop increased. A decrease in superheat may affect alumina dissolution, increasing risk of sludge formation. The decrease in current efficiency may be compensating part of the heat deficit originating from bottom lining deterioration.

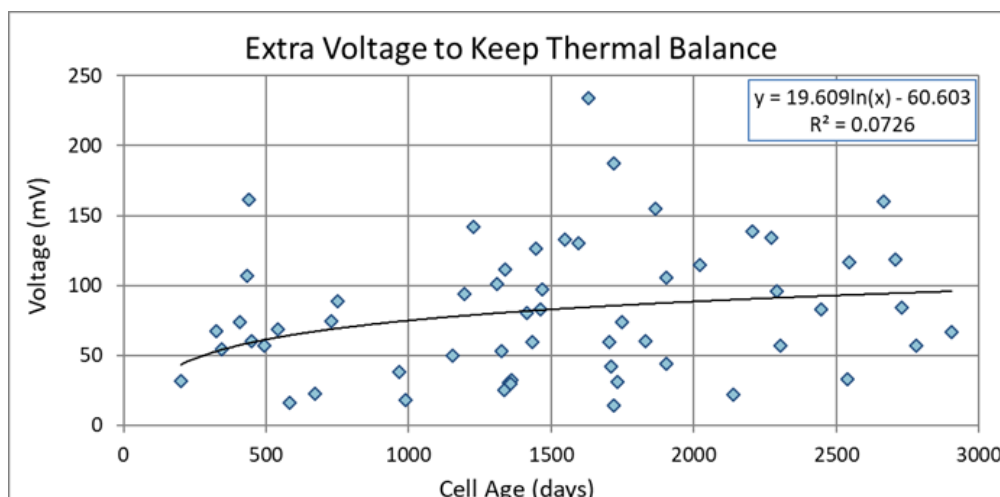


Figure 17. Extra cell voltage to compensate extra bottom heat losses for existing cells.

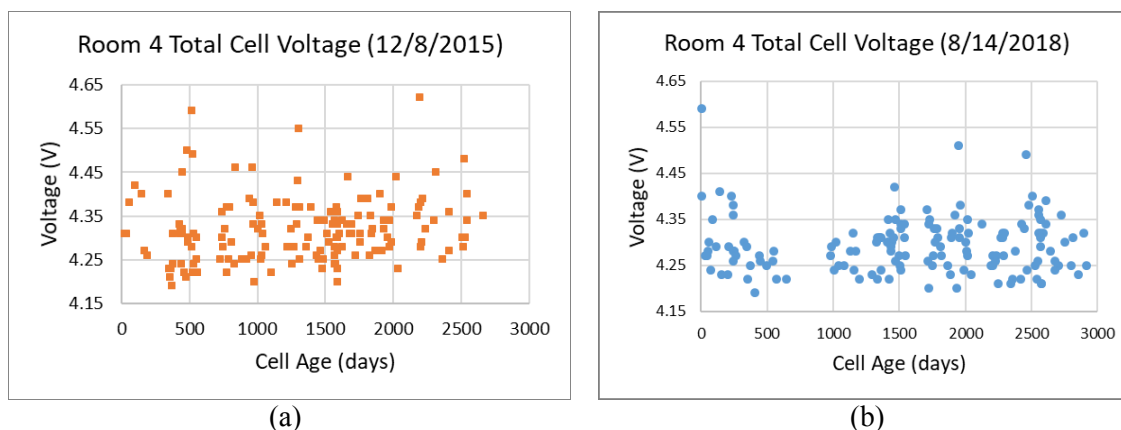


Figure 18. Room 4 cell voltage on 8 December 2015 (a) and 14 August 2018 (b).

The cell voltage is related to transient factors, such as the need to reduce instability, to reduce sludge, increase or decrease temperature, etc. Figure 19 shows that there is no correlation between the measured heat flux and the total cell voltage in the same day of the measurements. This means that other factors had more impact on the total voltage at the time of the measurements.

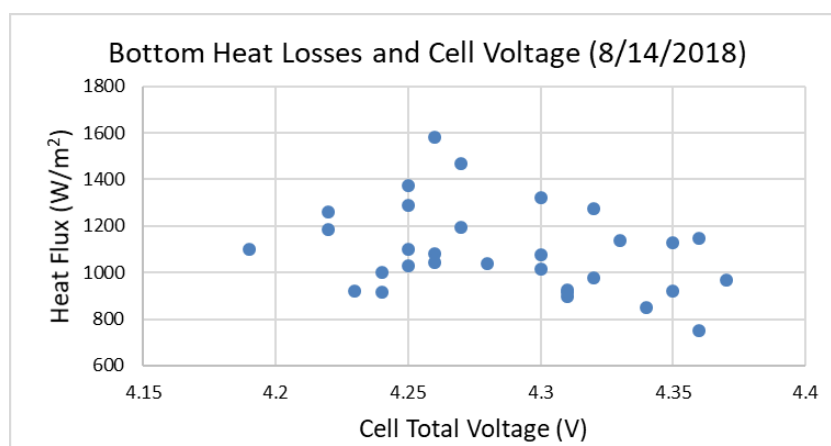


Figure 19. Bottom heat losses and cell voltage on 14 August 2018.

## 6. Sludge and Hard Muck

At CBA the Soderberg cells are fed by breaking the side crust and adding a large amount of alumina at the time. Much of the alumina that is not dissolved in the bath after the feeding is deposited on the top of cathode panel, making the sludge. Only the sludge liquid phase has the ability to return alumina to the bath through the process called "back feeding".

The sludge solidification temperature is 954.6 °C, considering a composition of 3 %  $\text{AlF}_3$  and 5 %  $\text{CaF}_2$  (typical measured sludge composition) and saturated in alumina [7]. If the cell operates with high  $\text{AlF}_3$ , the liquidus temperature is lower and very close to the solidification point of the sludge. Any oscillation in bath chemistry can cause formation of solid sludge and stop the process of "back feeding" [8]. The solid sludge may not be re-dissolved and progressive accumulation can occur.

It is known experimentally that bath with higher acidity has lower solubility of the liquid aluminum [9], reducing the re-oxidation rate of aluminum. However operating side-break cells with high  $\text{AlF}_3$  will increase the risk of liquid and solid sludge.

The cells are running at 10 %  $\text{AlF}_3$ , which is a relatively high value considering a side-break technology. Also, the bath temperature should be kept below 962 °C to avoid anode issues like carbon dust. The operational window for the bath temperature is then very narrow. The risk of having the bath temperature below the sludge solidification temperature is high.

Some of the cells have the sub-cathodic lining damaged, which reduces its thermal resistance, increasing heat flux and the risk of the top of the cathode reaching temperature below 955 °C. Figure 20(a) shows the bath temperature of Room 4 in 2018. We can notice around 17 % of cells have bath temperature below 955 °C.

All these conditions together may explain why large volumes of solid sludge phase and alpha alumina (corundum) are found in CBA cells - Figure 20(b).

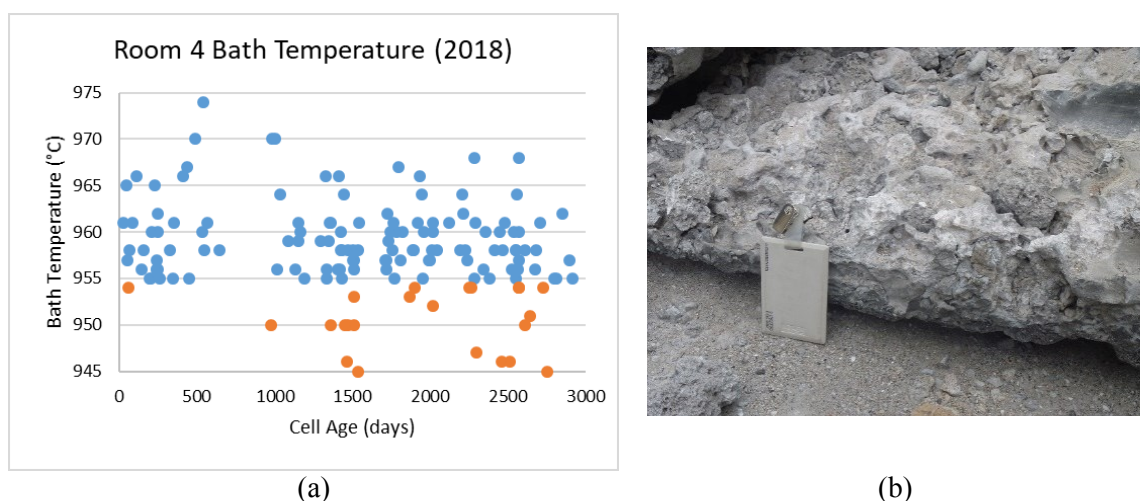


**Figure 20. Room 4 cell bath temperature on 15 August 2018 (a) and hard muck removed from the cathode top of the Cell 1639 (b).**



## 7. Conclusion

Numerical model, autopsies and internal thermocouple measurements confirm the hypotheses of an over insulated bottom lining by design at CBA cells. Due to this over insulated bottom and the use of low silica refractory bricks, a diffusion barrier did not form in the bottom of the CBA cells. This leads to a contamination of the insulation thus increasing the heat loss from the cells over time. The cells were not equally affected, as the measurements of heat flux showed. Also, variations were found in the same cell. Even though the cell materials and start-up are the same, it is not known why the cells have different behaviour. It is possible that differences in preheat temperature distribution lead to cracks making the infiltration rate non-uniform [10].

When the sub-cathodic insulation is destroyed it is necessary to operate the cell with a higher voltage to compensate the extra heat losses. The cell is kept in thermal balance adjusting the ACD to generate the proper heat to compensate the heat losses. Although no correlation was found, one of the reasons for the dispersion of the voltage necessary to maintain the thermal balance must be related to the degree of contamination of the lining, which is not uniform even in the same cell.

The hard muck usually found in the CBA cells is directly related to the sludge at the cathode top. CBA cells are prone to form sludge due to their side-break feeding, high  $\text{AlF}_3$  and deteriorated sub-cathodic lining. Then the sludge becomes hard muck when the cathode top reaches the eutectic temperature for alumina.

The non-uniform distribution of hard muck, liquid and solid sludge over the cathode top generates electrical perturbation leading to magnetic instabilities which results in energy consumption increase. The accumulation of hard muck reduces the cell cavity resulting in sidewall bath infiltration and tap-out.

So far, the test cells using the stainless-steel barrier seem to be preventing bath components and sodium migration into the insulation bricks. Heat flow measurement done on three occasions did not show significant increase of heat loss over cell life. The use of steel plates as a diffusion barrier in an over-insulated bottom will only postpone the destruction of the bottom insulation [10]. However, we expect that the stainless-steel plates will last longer than the low carbon steel due to their better corrosion resistance.

Regarding the cost, when steel plates are used as a diffusion barrier approximately 100 kg of low carbon steel per  $\text{m}^2$  of cell bottom area are used. The test cells used only around 25 kg of stainless steel per  $\text{m}^2$ . So, although the stainless steel (AISI 304) cost is 3.5 times higher than the cost of low carbon steel, the cost of this design is below the one using carbon steel. In the test cells around 850 kg of stainless steel were used which cost around USD 4 500 per cell in 2015.

If we consider the average gain of cell voltage being 100 mV over a 3 000 days cell life, the total energy saving will be around 920 MWh at 128 kA of cell current. If the energy cost is 30 USD/MWh the total savings will be around 27 000 USD. This is only the direct gain not considering gains in cell stability, reduction of sidewall tap-outs, etc.

## 8. References

1. Kati Tschöpe, Degradation of cathode lining in Hall-Hèroult cells, Ph.D. Thesis, Department of Materials Science and Engineering, *Norwegian University of Science and Technology*, Trondheim, 2010.
2. Asbjørn Solheim, Christian Schøning, and Egil Skybakmoen, Reactions in the bottom lining of aluminium reduction cells. *Light Metals* 2010, 877-882.

3. Jean C. Pardo et al., Cathode performance evaluation at Votorantim Metais – CBA, *Light Metals* 2012, 1241-1246.
4. Claude Allaire, Efficiency of steel plate barriers in aluminum reduction cell potlining refractories, *Journal of the Canadian Ceramic Society*, Vol 63, No.2, May 1994.
5. B. Garnier, F. Lanzetta and S. Gomès, Measurements with contact in heat transfer: principles, implementation and pitfalls, *Thermal Measurements and Inverse Techniques – 6<sup>th</sup> Edition*, Biarritz, March 1 - 6, 2015.
6. Pierre Homsy, Jean-Michel Peyneau and Michel Reverdy, Overview of process control in reduction cells and potlines; *Light Metals* 2000, 223-230.
7. Pierre-Yves Geay, Barry J. Welch and Pierre Homsy, Sludge in operating aluminium smelting cells, *Light Metals* 2001, 541-547.
8. Daniel Whitfield, Aspects of temperature in aluminium smelting, PhD Thesis, School of Chemical Engineering, Faculty of Engineering, *University of New South Wales*, Sydney-Australia, 2003.
9. Xiangwen Wang, Ray D. Peterson, and Nolan E. Richards, Dissolved metals in cryolitic melts, *Light Metals* 1991, 323-330.
10. Morten Sørli and Harald A. Øye, Cathodes in aluminium electrolysis, *Aluminium-Verlag*, 3<sup>rd</sup> Edition, 2010.